Asp537 and Asp812 in Bacteriophage T7 RNA Polymerase as Metal Ion-Binding Sites Studied by EPR, Flow-Dialysis, and Transcription†

A-Young Moon Woody,*,‡ Sandra S. Eaton,§ Patricia A. Osumi-Davis,‡ and Robert W. Woody‡

Department of Biochemistry and Molecular Biology, Colorado State University, Fort Collins, Colorado 80523, and Department of Chemistry, University of Denver, Denver, Colorado 80208

Received August 28, 1995; Revised Manuscript Received November 2, 1995⊗

ABSTRACT: Asp537 and Asp812 are essential in the catalytic mechanism of T7 RNA polymerase. The mutants D537N and D812N have no detectable activity whereas the mutants D537E and D812E have significantly reduced activity relative to the wild-type. The hypothesis that these two amino acids act as metal-binding ligands has been tested using EPR with Mn^{2+} as the metal ion. Mn^{2+} is able to substitute for Mg^{2+} in transcription by T7 RNAP on templates containing the T7 promoter. Mg^{2+} and Mn^{2+} compete for binding sites, with the former having lower affinity. Mn^{2+} binding to the wild-type enzyme and the mutants D537N, D812N, D537E, D812E, and Y649F was measured over the concentration range of 25 μM to 1.5 mM. The data were analyzed by nonlinear least-squares fits to the binding isotherms, and the analysis gave approximately two Mn^{2+}-binding sites in all cases and a K_d for the wild-type of ∼340 μM. The K_d value for the mutant Y639F, in which Asp537 and Asp 812 are not mutated, is comparable to the value for the wild-type. Mn^{2+} binding to the double mutants, D537N/D812N and D537E/D812E, appears to be nonspecific. The K_d values of the Asp → Asn mutants are only 2−5 times larger than the value for the wild-type, in contrast to the drastic diminution of enzymatic activity in the mutants. The geometry of metal binding to these Asp residues may be crucial in determining the catalytic competence. Mn^{2+} binding to the wild-type enzyme in the presence of nucleotides, measured by flow dialysis, is characterized by two Mn^{2+}-binding sites with a K_d value of ca. 150 μM. The similarity in values of K_d with and without nucleotide suggests that nucleotides do not have a drastic effect on Mn^{2+} binding. Our results indicate that monodentate carboxylate oxygens of both conserved Asp residues bridge the two metal ions.

The transcription process in which RNA is synthesized on a DNA template plays a central role in biology, and RNA polymerase is the enzyme responsible for the trnascription process. Understanding the mechanism of RNA polymerase-catalyzed RNA synthesis will enhance our basic knowledge of gene expression. The RNA polymerase from T7 bacteriophage is well suited for mechanistic studies on many aspects of transcription because it is a single-subunit enzyme (99 kDa) and can be overproduced (Davanloo *et al*., 1984) for biochemical and biophysical studies. In recent years, there has been steady progress in elucidating the active site of this enzyme, an imperative in understanding the mechanism of RNA synthesis. A functional group responsible for promoter specificity has been identified (Raskin *et al*., 1992), and several catalytically essential and significant functional groups have been identified through site-directed mutagenesis studies (Osumi-Davis *et al*., 1992, 1994; Bonner *et al*., 1992, 1994) and deletion studies (Mookhtiar *et al*., 1991). The participation of several regions of the polypeptide chain to form the active site has been indicated (Delarue *et al*., 1991; Knoll *et al*., 1992). The crystal structure of the enzyme solved at 3.3 Å (Sousa *et al*., 1993) has confirmed the biochemical studies mentioned above, and has shown the layout of the important functional groups. It also has highlighted the similarities of the putative active sites among the polymerases whose X-ray structures have been determined (Ollis *et al*., 1985; Kohlstaedt *et al*., 1992; Jacobo-Molina *et al*., 1993; Sousa *et al*., 1993; Davies *et al*., 1994; Pelletier *et al*., 1994).

How these functionally significant amino acids, Asp537, Lys631, Tyr639, His811, and Asp812, participate in carrying out the transcription process has yet to be elucidated. Two of the residues (Asp537 and Asp812) play especially critical roles because if either is substituted by Asn, a neutral but isosteric amino acid, the enzyme is totally inactive (Osumi-Davis *et al*., 1992). The aim of the present work is to test the hypothesis that Asp 537 and/or Asp 812 serve as ligands for one or more divalent cations (normally Mg^{2+}), either as the free metal ion or complexed with the substrates, nucleoside triphosphates (NTPs). Asp was mutated to Asn or Glu. In each case, the replacement side chain in the mutant has the potential to bind to a metal ion, but the changes in charge for Asn and the longer side chain of Glu are expected to impact the dissociation constants if Asp537 or Asp 812 coordinates to Mn^{2+}/Mg^{2+}. CD, fluorescence, and calorimetric studies of these mutants found no detectable impact of these mutations on protein folding or stability (Osumi-Davis *et al*., 1994). EPR, flow dialysis, and transcription assays have been used to examine metal ion binding. Many of the experiments have used Mn^{2+} in addition to, or instead of, Mg^{2+}. Mn^{2+} is paramagnetic and therefore gives rise to an electron paramagnetic resonance (EPR) signal, whereas Mg^{2+} has no EPR signal. In addition,

† Supported by NIH Grant GM-23697 and BRSG S07 RR07127 (A-Y.M.W. and R.W.W.) and NSF Shared Instrument Grant CHE-9318715 for purchase of the Bruker ESP380E (S.S.E.).

* Author to whom correspondence should be addressed.
‡ Colorado State University.
§ University of Denver.

⊗ Abstract published in *Advance ACS Abstracts,* January 1, 1996.

0006-2960/96/0435-144$12.00/0

although Mn^{2+} is somewhat larger than Mg^{2+}, it can take the place of Mg^{2+} in many biological reactions, including RNA synthesis.

EXPERIMENTAL PROCEDURES

Wild-Type and Mutant T7 RNA Polymerases. The methodology to produce the mutants has been described previously (Osumi-Davis *et al*., 1992). The purification of the wild-type and mutant enzymes was based on the procedure of Grodberg and Dunn (1988) with the following modifications. All traces of EDTA had to be eliminated in the case of Mn^{2+}-binding experiments. Therefore, the purification procedure was modified to exclude EDTA throughout the three column purification steps, although it was used in the initial lysis steps. This modification did not decrease the overall enzyme activity. The purified enzyme was stored in 50% glycerol−20 mM sodium phosphate, pH 7.8, containing 100 mM NaCl and 1 mM dithiothreitol (DTT). For EPR experiments, the enzyme in the storage buffer was filtered through a Biogel P-6DG desalting column, which was preequilibrated with 10 mM Tris-HCl, pH 8.0, containing 150 mM KCl (binding buffer) and was then concentrated to the desired level using Centricon microconcentrators (Amicon, Beverly, MA).

Buffers. For EPR and flow-dialysis experiments, binding buffer was used throughout the experiments to alleviate possible aggregation of T7 RNA polymerase and the Donnan effect that might arise at the concentration levels used. For transcription assays, 50 mM Tris-HCl, pH 7.9 (or 40 mM Tris-HCl, pH 7.9, plus 10 mM KCl), containing 1 mM DTT and 0.05−100 mM Mg^{2+} or 0.05−20 mM Mn^{2+} was used. Fresh stock solution of Mn^{2+} in binding buffer was prepared each day. Tris (ultra pure) was from United States Biochemical or from Sigma Chemicals. KCl (ACS certified) and $MgCl_2 \cdot 6H_2O$ (ACS certified) were from Fisher Scientific. $MnCl_2 \cdot 4H_2O$ (99.99%) was from Aldrich, and $MnCl_2 \cdot 4H_2O$ (AR, ACS certified) was from Mallinckrodt.

EPR. EPR spectra were recorded at 9.38 GHz on a Bruker ER200D or a Bruker ESP380E EPR spectrometer with a rectangular TE_{102} resonator containing a quartz variable-temperature dewar insert. EPR samples were contained in 0.4 × 4.0 mm flat slides supported in a thin-walled Teflon holder positioned with the 4.0 mm dimension perpendicular to the direction of the external magnetic field (Eaton & Eaton, 1977).

Spectrometer settings were 3350 G center field, 750 G sweep width, 1 min scan, 16 G magnetic field modulation amplitude at 100 kHz, and 20 mW microwave power. This microwave power does not cause saturation of the signal. The peak to peak line widths in the spectrum of Mn^{2+} in buffer are about 22G. The selection of 16 G modulation amplitude was a compromise between the need for improved signal-to-noise ratio for spectra at low concentrations and the desire to minimize line shape distortion by overmodulation. The modulation amplitude was held constant for all experiments. Two to eight scans were signal-averaged, and the background signal was subtracted. Within experimental uncertainty, there was no change in line width as a function of Mn^{2+} concentration, and, therefore, the average peak-to-peak height of the six hyperfine lines in the first-derivative spectra was used to relate the EPR signal intensity to free Mn^{2+} concentration. For each sample, to minimize the possible impact of errors due to reproducibility of sample positioning in the resonator, the spectrum was recorded twice, and the average peak height values for the two spectra were combined. Reproducibility of average peak heights was better than 3%. Plots of signal intensity vs Mn^{2+} concentration were linear.

Cohn and Townsend demonstrated the use of EPR spectra to determine Mn(II)-binding constants (Cohn & Townsend, 1954). They showed that the amplitude of peaks in the first-derivative spectrum of Mn^{2+} in aqueous solution was proportional to the concentration of Mn^{2+} and that coordination of the Mn^{2+} resulted in such extensive broadening of the EPR spectrum that bound Mn^{2+} was not detectable in the presence of free Mn^{2+}. It has been shown, for example, that addition of a 4-fold excess of $MnADP^-$ to a solution of Mn^{2+} had negligible impact on the EPR signal (O'Sullivan & Cohn, 1966). The extensive broadening of the signal for the bound Mn^{2+} is due to the increase in zero-field splitting and increase in tumbling correlation time relative to free Mn^{2+} (Meirovitch & Poupko, 1978). In this method for determining Mn^{2+}-binding constants for a protein, it is assumed that all decrease in the intensity of the EPR signal is due to coordination to the protein. The following control experiments were done in the absence of protein to check that components of the buffer or species added in binding constant studies did not cause changes in the Mn^{2+} signal. The peak heights and line widths in an aqueous solution of Mn^{2+} were indistinguishable from those in a spectrum at the same concentration in binding buffer. Addition of 150 mM KCl or 100 mM Mg^{2+} to the buffer had no detectable impact on the Mn^{2+} EPR spectrum. Protein-containing solutions were more viscous than controls, and, therefore, the impact of viscosity was checked by addition of glycerol to the buffer to make the relative viscosity of the buffer comparable to that of the protein solution containing 50−200 μM T7 RNA polymerase. Addition of 1−4% glycerol had no impact on the Mn^{2+} EPR signal, within experimental error.

Data Analysis. Standard curves correlating EPR signals and the concentrations of Mn^{2+} in binding buffer were constructed and used to determine the free Mn^{2+} concentration in the presence of protein. Each day a standard curve was constructed and compared with previous standard curves for reproducibility. A standard curve of EPR signal versus the concentration of $MnCl_2$ from an atomic absorption standard also was constructed as a control and compared with that obtained with reagent-grade $MnCl_2$. EPR spectra of varying concentrations of Mn^{2+} in the presence of T7 RNA polymerase were obtained, and the concentration of bound Mn^{2+} was calculated by subtracting the concentration of free Mn^{2+}, determined by EPR, from the total Mn^{2+} concentration. Based on the EPR data, binding isotherms (the number of metal ions bound per protein molecule versus free metal ions) were constructed, and a nonlinear least-squares fit was obtained using the Axum program (TriMetrix, Seattle, WA). The model for n equivalent noninteracting sites:

$$r = n[Mn^{2+}]_f/(K_d + [Mn^{2+}]_f) \quad (1)$$

gave a satisfactory fit. The model for two classes of noninteracting sites:

$$r = n_1[Mn^{2+}]_f/(K_{d1} + [Mn^{2+}]_f) + n_2[Mn^{2+}]_f/(K_{d2} + [Mn^{2+}]_f) \quad (2)$$

did not converge to a stable solution. The same procedure was applied to the binding isotherms constructed from flow-dialysis.

Flow Dialysis. The dissociation constants for Mn^{2+} in the presence of nucleotides were measured by the method of flow dialysis (Womack & Colowick, 1973) in which the rate of dialysis (proportional to the concentration of the free ligand) is measured in a flow cell until it reaches steady-state. The flow cell was constructed based on a design adapted for microscale applications (Muise & Holler, 1985). The cell consisted of an upper chamber (~200 μL capacity; 0.6 cm diameter, 0.8 cm height) and a lower chamber (~3.5 μL capacity; 0.15 cm in diameter, 0.2 cm in height), separated by a dialysis membrane (Spectra/Por, molecular weight cutoff 12 000−14 000). The lower chamber was connected to the pump and fraction collector and was flushed with the same buffer present in the upper chamber, at a rate of 200 μL/min. The cell was secured in a small water bath to keep the reaction temperature steady at 23 ± 1 °C, and the water temperature was monitored with a YSI telethermometer, Model 42SC (Yellow Springs Instruments, Inc., Yellow Springs, OH). The reaction solution in the upper chamber was 100 μL containing ca. 39−50 μM T7 RNA polymerase and 0.5 mM GTP in binding buffer. This solution was stirred with a tiny magnetic bar and titrated with a manganese cocktail of $^{54}Mn^{2+}$ and Mn^{2+} in binding buffer. As controls, titration experiments were performed as above in the absence of T7 RNA polymerase. Binding of Mn^{2+} to T7 RNA polymerase was followed by measuring the amount of radioactivity that became nondiffusable due to binding to the enzyme and was analyzed, with some modifications, based on the method of Norby and Jensen (1988). For a given concentration of Mn^{2+}, 15 eluent samples per titration were collected in a period of 15 min. Exploratory experiments demonstrated that 15 min was adequate for the dialysis to achieve steady-state. The number of titrations per fresh aliquot of enzyme was limited to 1−4 (15−60 min) to minimize any deleterious effects such as denaturation of enzyme or volume changes that might arise. One milliliter of the scintillant Ecoscint A (National Diagnostics, Atlanta, GA) was added to each tube, the tubes were well mixed, and counted in a Beckman LS7800 liquid scintillation counter (Beckman Instruments, Inc., Irvine, CA).

Construction of Binding Isotherm from Flow Dialysis Data. In order to construct the binding isotherm, several independent experiments were performed to obtain the desired range of Mn^{2+} concentrations and to assess reproducibility. Free Mn^{2+} concentration in the reaction cell containing protein was calculated from the radioactivity in the cell as follows. The rate of dialysis in the absence of protein was established by successive titrations of buffer plus 0.5 mM GTP with a radioactively labeled Mn^{2+} solution of known concentration and specific activity. The plot of the activity eluted at steady-state, $(cpm)_{isb}$, versus the radioactivity in the reaction cell at each titration point, $(cpm)_{ib}$, gives a slope f (eq 3), from which the expected radioactivity, $(cpm)_{isp}$, eluted at steady-state can be calculated from a given initial radioactivity, $(cpm)_{ip}$, in the reaction cell (eq 4). The radioactivity eluted at steady-state for a given titration in the presence of protein, $(cpm)_{sp}$, is determined experimentally. The concentration of free Mn^{2+}, $[Mn^{2+}]_f$, is calculated using eq 5. $[Mn]_i$ is the initial Mn^{2+} concentration at

$$f = (cpm)_{isb}/(cpm)_{ib} \quad (3)$$

$$(cpm)_{isp} = (cpm)_{ip} f \quad (4)$$

$$[Mn^{2+}]_f = [(cpm)_{sp}/(cpm)_{isp}][Mn^{2+}]_i \quad (5)$$

successive titration points corrected for diffusion and volume increase. From the free Mn^{2+} concentration and the known initial concentration of Mn^{2+} and T7 RNA polymerase, the bound Mn^{2+} concentration can be calculated, and a binding isotherm can be constructed. In calculations of Mn^{2+} bound, corrections were made for the volume increase due to the addition of titrant, and the loss of Mn^{2+} due to elution during the 15 min dialysis. Under our flow dialysis conditions in which the GTP concentration was kept at 0.5 mM and the Mn^{2+} concentration was varied from 0 to 350 μM, most of the Mn^{2+} will be complexed with GTP since the K_d of the Mn^{2+}−ATP complex is ~14 μM (Mildvan & Cohn, 1966). The rate of Mn^{2+} elution across the dialysis membrane (MW cutoff 12 000−14 000) was the same, within experimental uncertainty, in the presence of 0, 0.1, or 0.5 mM GTP. The effect of the protein on the rate of dialysis was also addressed: (1) the ionic strength of the buffer was high enough to alleviate the Donnan effect, and (2) variation of the enzyme concentration from 39 to 90 μM did not have an observable effect on the rate of elution.

Transcription Assay and Steady-State Kinetics. The procedures for the transcription assay and steady-state kinetics have been described (Osumi-Davis *et al*., 1992, 1994). Specific conditions are described in the legends for Figure 5 and for Tables 1 and 2.

Templates and Radioactive Nucleotides. Steady-state kinetic parameters were obtained using 22 base pair (bp) oligonucleotide templates containing the T7 promoter plus five additional nucleotides: 5′-TAATACGACTCACTATAGGACT-3′ is the nontemplate strand of template A; 5′-TAATACGACTCACTATAGGTAC-3′ is the nontemplate strand of template U. These oligonucleotides were synthesized in the Macromolecular Resource Facility at Colorado State University.

pT713 plasmid DNA linearized with endonuclease *Bam*HI was used as a template to study the effect of Mn^{2+} on the synthesis of 60 nt run-off transcripts.

The radioactive nucleotides [α-^{32}P]GTP, [α-^{32}P]UTP, [α-^{32}P]ATP, and [α-^{32}P]CTP were purchased from Amersham Life Science Inc. (Arlington Heights, IL).

RESULTS

EPR Probe for Residues Asp537 and Asp812 as Metal-Binding Sites. We have studied Mn^{2+} binding to the wild-type T7 RNA polymerase and to mutants in which Asp537 and/or Asp812 have been replaced by Asn or Glu using EPR at room temperature (~23 °C). The metal ion normally used for T7 RNA polymerase activity is Mg^{2+}, but it is EPR-silent because its orbitals are filled, whereas Mn^{2+} has five unpaired electrons in 3d orbitals and is EPR-active. Mn^{2+} can substitute for Mg^{2+} in the transcription process catalyzed by T7 RNA polymerase (see next section). Free Mn^{2+} gives an EPR signal, but the signal for protein-bound Mn^{2+} is so

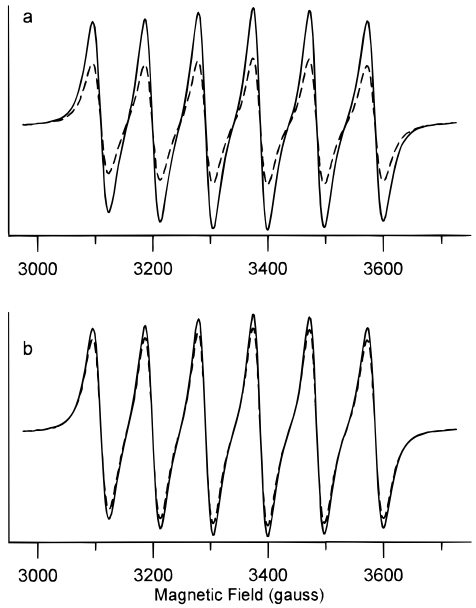

FIGURE 1: EPR spectra of Mn^{2+} in the absence and presence of wild-type and mutant D537N in 10 mM Tris-HCl, pH 8.0, containing 150 mM KCl at ~23 °C. (a) Wild-type. Solid curve, Mn^{2+} alone (150 μM); dashed curve, Mn^{2+} (150 μM) plus wild-type enzyme (217 μM). (b) D537N. Solid curve, Mn^{2+} alone (150 μM); dashed curve, Mn^{2+} (150 μM) plus mutant D537N (170 μM).

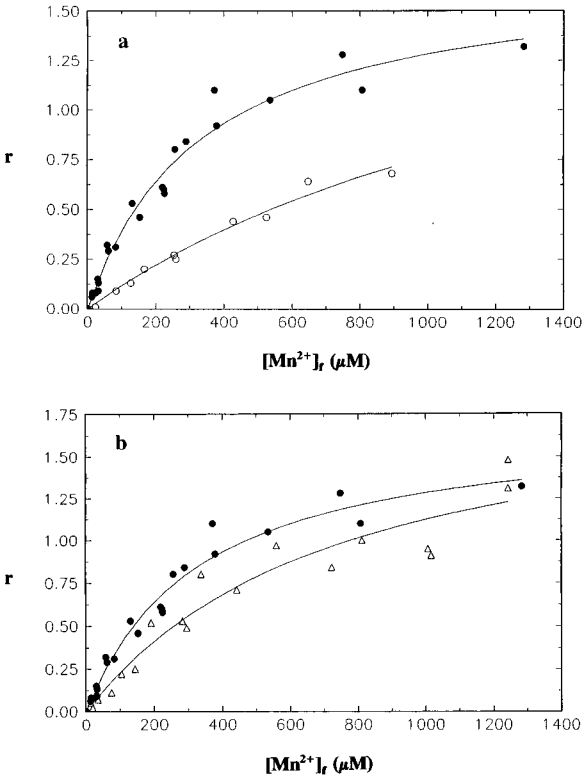

FIGURE 2: Isotherms of Mn^{2+} binding to the wild-type enzyme and mutants D537N and D812N in 10 mM Tris-HCl, pH 8.0, containing 150 mM KCl at ~23 °C. The variable *r* is the number of Mn^{2+} bound per protein molecule. (a) Wild-type (solid circles) and D537N (empty circles). (b) Wild-type (solid circles) and D812N (empty triangles).

broad that it is undetectable under the conditions used to observe the free Mn^{2+} (see Experimental Procedures), and, therefore, EPR can be used conveniently to construct the isotherm for metal ion binding to T7 RNA polymerase. The Mn^{2+} EPR spectra in the presence and absence of the wild-type and mutant D537N enzymes are shown in Figure 1 as examples, and the binding isotherms of the wild-type, D537N, and D812N mutant enzymes constructed from the EPR data are shown in Figure 2. The data were analyzed by nonlinear least-squares fits to the binding isotherms as described under Experimental Procedures, and the results are tabulated in Table 1 for the wild-type and for mutants with single amino acid mutations, D537N, D812N, D537E, and D812E. The results show two Mn^{2+}-binding sites in all cases, and the changes in K_d values observed on mutation of either Asp537 or Asp812 suggest that both Asp side chains participate in binding to both Mn^{2+}. The relative standard deviations of the K_d values range from 14% to 32%. These deviations seem somewhat large, but they are not unreasonable in view of the fact that (1) the protein-bound Mn^{2+} concentrations were obtained not from direct measurements but calculated as the difference between the total concentration of Mn^{2+} and the observed concentration of free Mn^{2+} as described under Experimental Procedures and (2) the preparation of the sample solutions involved multiple pipetting of small volumes. Scatchard plots (not shown) show a straight line within experimental error, consistent with a single intrinsic dissociation constant. However, it must be noted that even if two intrinsic dissociation constants were different by an order of magnitude, because of experimental scatter, it would be difficult to observe detectable deviations from linearity (see Discussion). The double mutants, D537N/D812N and D537E/D812E, with no detectable enzymatic activity, show what appears to be nonspecific binding only (data not shown).

EPR experiments on Mn^{2+} binding to the Y639F mutant were performed as a control since this mutant does not

Table 1: Binding of Mn^{2+} to Wild-Type and Mutant T7 RNA Polymerases Measured by EPR[a]

enzyme	n[b]	K_d[c] (μM)
WT	1.7 ± 0.1	339 ± 46
D537N	2.0 ± 0.5	1601 ± 518
D812N	2.0 ± 0.3	755 ± 239
D537E	1.8 ± 0.2	690 ± 116
D812E	2.4 ± 0.4	1136 ± 316
Y639F	1.7 ± 0.1	315 ± 51

[a] Mn^{2+}-binding reaction mixture contained 10 mM Tris-HCl, pH 8.0, containing 150−200 μM enzyme, and varying Mn^{2+} from 25 to 1500 μM. K_d and n values for n equivalent noninteracting sites were obtained from nonlinear least-squares fits to the binding isotherms. [b] Number of metal ions bound per protein molecule. [c] Dissociation constant.

involve either of the two Asp residues (Asp 537 and Asp 812) and its enzymatic activity is comparable to that of the wild-type. A nonlinear least-squares fit to the binding isotherm (Figure 3) gives $n = 1.7 \pm 0.1$ and $K_d = 315 \pm 51$ μM (Table 1). These values are, within experimental error, identical to those for the wild-type enzyme, which adds further evidence that the two Asp residues participate in metal binding.

Figure 4 shows a possible model of Mn^{2+} binding to the Asp residue in the wild-type enzyme and the Asn residue in the mutant D537N or D812N that is compatible with our EPR data. This model shows, for the wild-type enzyme, the two metal ions bridged by a monodentate carboxylate oxygen of Asp537 and by a monodentate oxygen of Asp812. For the Asn mutants, the amide oxygen replaces one of the monodentate carboxylate oxygen (see Discussion). In the case of the mutants D537N and D812N, the partial negative

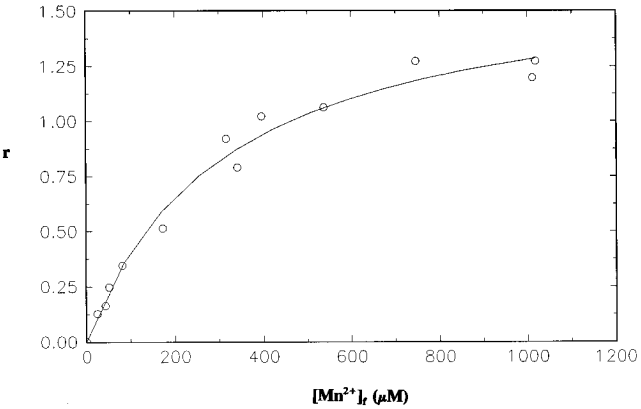

FIGURE 3: Isotherm of Mn^{2+} binding to Y639F mutant obtained by EPR in 10 mM Tris-HCl, pH 8.0, containing 150 mM KCl at ~23 °C.

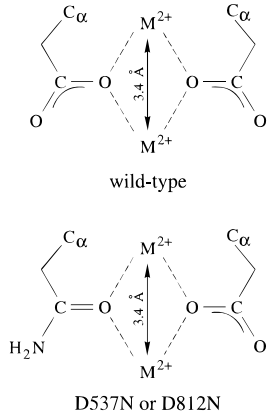

FIGURE 4: Possible models for the Asp and Asn ligand−metal interactions. The two metal ions are bridged by monodentate carboxylate oxygens of Asp537 and Asp812 for the wild-type, and for the Asp → Asn mutants, an amide carbonyl oxygen replaces one of the monodentate carboxylate oxygens.

charge on the oxygen of the amide will be less than that of the aspartate oxygen in the wild-type enzyme, and this will decrease the affinity of Mn^{2+} for these mutants, consistent with our EPR data. In the case of D537E and D812E, although two carboxylates are available, the lengthened side chain decreases the affinity of these mutants for Mn^{2+}, probably due to less than optimal binding site geometry.

The results in Table 1 show that the K_d values for the mutants D537E and D812N are not very different from each other and are at most twice the value for the wild-type. Even the single mutant most strongly deviating from the wild-type, D537N, has a K_d value which is only 4−5 times larger than that of the wild-type. The changes were much larger for the double mutants. Despite these relatively small decreases in metal ion affinity, the mutants D537N and D812N show no enzymatic activity (Osumi-Davis et al., 1992, 1994; see below and Discussion).

Mn^{2+} as a Transcription Activator. Mn^{2+} is able to substitute for Mg^{2+} in the synthesis of short oligonucleotide transcripts on 22 bp templates containing the T7 promoter, and of longer transcripts on pT713-*Bam*HI plasmid DNA, catalyzed by T7 RNA polymerase. The effects of Mg^{2+} and Mn^{2+} concentration on the synthesis of trimer GGU and 60 nt RNA by the wild-type enzyme are shown in Figure 5. Assays at various times ensure that we are working in the linear range of production of the transcripts. Mn^{2+} and Mg^{2+} concentration-dependent transcription activation also was

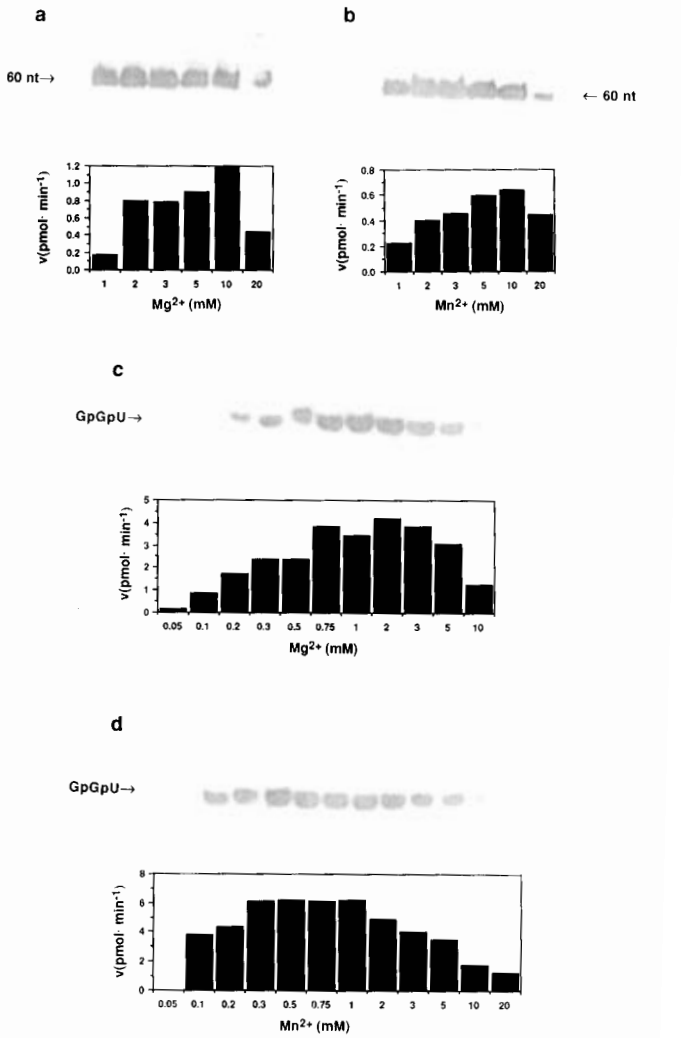

FIGURE 5: Autoradiogram of 25% urea−PAGE of trimer synthesis (GpGpU) and 60 nt run-off transcripts with wild-type enzyme at various metal concentrations, and a profile of the activity at those same concentrations. (a and b) Synthesis of 60 nt run-off transcript in the presence of 1.0−20 mM Mg^{2+} and Mn^{2+}, respectively. The synthesis was carried out in 10 mM Tris-HCl, pH 7.9, 50 mM KCl, 1 mM DTT, 20 nM enzyme, 50 nM pT713 *Bam*HI-linearized DNA, 5 μCi of [α-^{32}P]UTP, 400 μM GTP, and 50 μM each of ATP, CTP, and UTP, at 37 °C for 5 min. (c and d) Synthesis of GpGpU in the presence of 0.05−10 mM Mg^{2+} and Mn^{2+}, respectively. The synthesis was carried out in the same buffer as in panels a and b, containing 20 nM enzyme, 200 nM template U (5′-TAATAC-GACTCACTATAGGTAC-3′), 2−4 μCi of [α-^{32}P]UTP, 400 μM GpG, and 100 μM UTP at 37 °C for 5 min. The bands of interest were quantitated on a Molecular Dynamics PhosphorImager SP. Estimated errors are ±5%.

investigated for the synthesis of pentamer GGACU by the wild-type and the mutants, D537E and D812E, and the results are shown in Tables 2 and 3. The optimum concentration of Mn^{2+} for the wild-type enzyme-catalyzed transcription is ~1 mM, whereas that for the two Asp → Glu mutants is ~2 mM. These results are consistent with the binding data obtained by EPR, according to which K_d values for the interaction of Mn^{2+} with the mutants D537E and D812E are higher than that for the wild-type (Table 1). In all cases examined, the Mn^{2+} concentration necessary for the optimum enzymatic activity is less than the Mg^{2+} concentration required for optimum activity. The mutants D537N and D812N do not have enzymatic activity for the synthesis of trimer, pentamer, or 87 nt RNA in the presence of 0.5−20 mM Mn^{2+} or 0.5−100 mM Mg^{2+}. We have also examined

Table 2: Synthesis of Pentamer GGACU Activated by Mn^{2+} [a]

	$(k_{cat})_{app}$ (min^{-1})[b]		
Mn^{2+} (mM)	WT	D537E	D812E
0.5	2.1 ± 0.2	1.8 ± 0.2	0.9 ± 0.2
1.0	8.1 ± 1.4	5.2 ± 0.4	7.6 ± 3.0
2.0	6.1 ± 1.7	5.7 ± 0.7	8.2 ± 3.0
3.0	4.9 ± 2.5	5.6 ± 0.8	6.5 ± 2.5
10.0	3.2 ± 0.6	3.0 ± 0.7	1.5 ± 0.3

[a] Enzyme assay solution contained 0.4−1.0 mM GpG, 100 μM ATP and CTP, 400 μM UTP, 20 nM enzyme, 200 nM template A (5′-TAATACGACTCACTA*G*GACT-3′), varying $MnCl_2$, 40 mM Tris-HCl, pH 8.0, 10 mM KCl, and 1 mM DTT. [b] The $(k_{cat})_{app}$ values are quantitated from experimental data (25% urea−PAGE) by PhosphorImager SP.

Table 3: Synthesis of Pentamer GGACU Activated by Mg^{2+} [a]

	$(k_{cat})_{app}$ (min^{-1})[b]		
Mg^{2+} (mM)	WT	D537E	D812E
1.0	4.0 ± 0.2	2.9 ± 0.4	1.2 ± 0.4
2.0	6.5 ± 0.2	4.7 ± 0.1	1.9 ± 0.6
3.0	7.2 ± 0.1	4.5 ± 0.2	2.7 ± 0.5
5.0	6.4 ± 0.2	4.6 ± 0.3	3.0 ± 0.1
10.0	5.1 ± 0.2	3.6 ± 0.1	3.5 ± 0.7
20.0	3.6 ± 0.6	3.5 ± 0.2	3.9 ± 0.2
30.0	1.8 ± 0.3	2.4 ± 0.1	2.9 ± 0.3

[a] Experimental conditions were the same as in Table 2 except that Mg^{2+} was used. [b] The $(k_{cat})_{app}$ values are determined as in Table 2.

Table 4: Synthesis of Pentamer GGACU Activated by Mg^{2+} and Mn^{2+} in the Same Reaction Mixture[a]

metal ions		$(k_{cat})_{app}$ (min^{-1})[b]
Mg^{2+} (mM)	Mn^{2+} (mM)	for WT
30.0	0.0	2.3 ± 1.1
30.0	0.001	2.3 ± 1.0
30.0	0.01	1.7 ± 0.3
30.0	1.0	2.8 ± 0.7
30.0	10.0	3.1 ± 0.6
0.0	30.0	2.7 ± 0.7
20.0	0.0	2.6 ± 1.0
20.0	1.0	2.6 ± 1.0
20.0	10.0	2.4 ± 0.2

[a] Experimental conditions were the same as in Table 2 except that both Mg^{2+} and Mn^{2+} were present in the same reaction solution. [b] The $(k_{cat})_{app}$ values are determined as in Table 2.

the effect of Mg^{2+} and Mn^{2+} in the same reaction mixture on the synthesis of GGACU catalyzed by the wild-type enzyme, and the results are tabulated in Table 4. The results illustrate that at 30 mM Mg^{2+}, the value of $(k_{cat})_{app}$ increases slightly upon the addition of 1 and 10 mM Mn^{2+} but the value of $(k_{cat})_{app}$ is largely determined by the presence of 30 mM Mg^{2+}. This is most clearly illustrated by the fact that 1 mM Mn^{2+} leads to a $(k_{cat})_{app}$ of 8.1 min^{-1}, and 30 mM Mg^{2+} gives 1.8 min^{-1} (Table 3), whereas 1 mM Mn^{2+} plus 30 mM Mg^{2+} gives 2.8 min^{-1} (Table 4). These results are consistent with those in Figure 6 showing that at 200 μM Mn^{2+} most of the bound Mn^{2+} are displaced by Mg^{2+} at 30 mM, and with the results in Tables 2 and 4 showing that the effectiveness of Mn^{2+} as a transcription activator is diminished at high concentrations (10 and 30 mM).

Mg^{2+} as a Competitor to Mn^{2+} Binding by EPR. In the previous section, it is shown that Mn^{2+} activates transcription as well as Mg^{2+}, if not better. Competition experiments show that Mg^{2+} competes with Mn^{2+} but at $[Mg^{2+}]/[Mn^{2+}] \gg 1$ (Figure 6). The mathematical model for two ligands

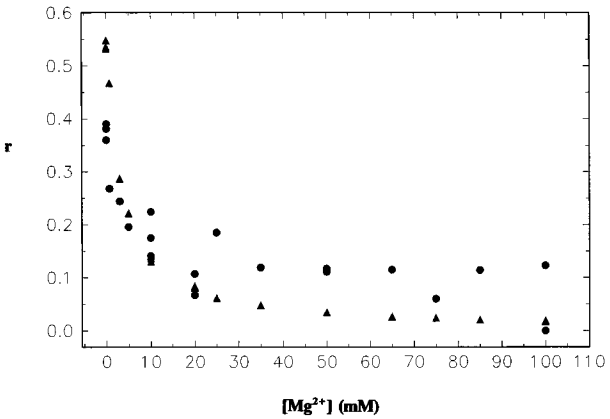

FIGURE 6: Competition of Mg^{2+} with Mn^{2+} for binding to T7 RNA polymerase. The number of Mn^{2+} bound to the wild-type enzyme measured by EPR in 10 mM Tris-HCl, pH 8.0, containing 150 mM KCl at ~23 °C is plotted against Mg^{2+} concentration (solid circles). T7 RNA polymerase and Mn^{2+} concentrations were kept at 200 μM, and Mg^{2+} concentration was varied from 0 to 100 mM. Our fit to the mathematical model for the two ligands binding to a single class of binding sites is shown as solid triangles.

binding to a single class of binding sites (Munsen, 1983) was used to fit our data, and the results are displayed along with the experimental data in Figure 6. The K_d value of ~2 mM for Mg^{2+} gives the best fit to the data, judging from the sum of the squares of the deviations between the calculated and experimentally obtained values of r for various values of K_d. The Mn^{2+} concentration was held at 200 μM. The larger deviations between the calculated and experimental values of r (Figure 6) at higher Mg^{2+} concentrations are attributable to larger experimental errors in determining increments in free Mn^{2+}. At higher Mg^{2+} concentrations, additional Mg^{2+} causes a small change in free Mn^{2+} which is difficult to measure accurately. The larger value of K_d for Mg^{2+} than Mn^{2+} is in agreement with the transcription data where the optimum concentration for Mg^{2+} is higher than that of Mn^{2+} (Figure 5). These observations are consistent with known differences between binding constants for the two metal ions (Irving & Williams, 1953): a given ligand generally binds to Mn^{2+} more tightly than to Mg^{2+}.

Mn^{2+} Binding Measured by Flow-Dialysis. Since it would be difficult to distinguish binding of Mn^{2+} to nucleotide from Mn^{2+} binding to protein, EPR experiments were limited to obtaining data on the binary interaction of Mn^{2+} and the enzyme. We measured the binding of Mn^{2+} in the presence of nucleotides to the wild-type enzyme using a flow-dialysis technique as described under Experimental Procedures. The isotherm for Mn^{2+} binding to the wild-type enzyme in the presence of 0.5 mM GTP was constructed from several independent experiments, and is shown in Figure 7. The nonlinear least-squares fit to this binding isotherm gave $n = 2.3 \pm 0.4$ and $K_d = 148 \pm 48$ μM, indicating somewhat tighter binding but not a drastic reduction in K_d. The experimental results obtained using flow-dialysis on wild-type enzyme in the absence of 0.5 mM GTP are displayed along with the data obtained by EPR in Figure 8. The standard deviations resulting from the EPR measurements are denoted with dotted curves to show the uncertainty due to experimental scatter. This figure shows that the r values obtained using flow-dialysis are a little higher, even in the absence of 0.5 mM GTP, than those obtained using EPR. Thus, in light of these observations, one can conclude that

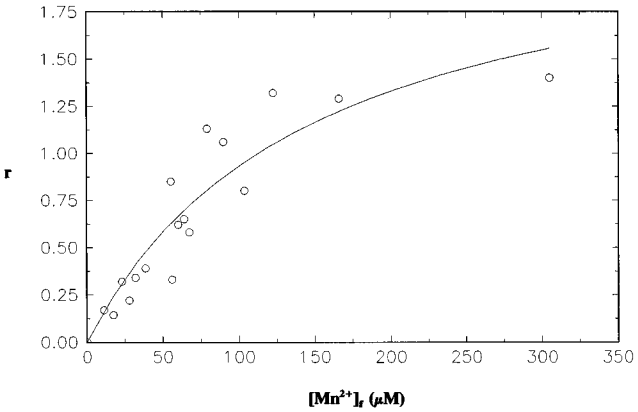

FIGURE 7: Binding isotherm constructed from flow-dialysis experiments on Mn^{2+} binding to 50 μM wild-type enzyme in the presence of 0.5 mM GTP in 10 mM Tris-HCl, pH 8.0, containing 150 mM KCl at ~23 °C.

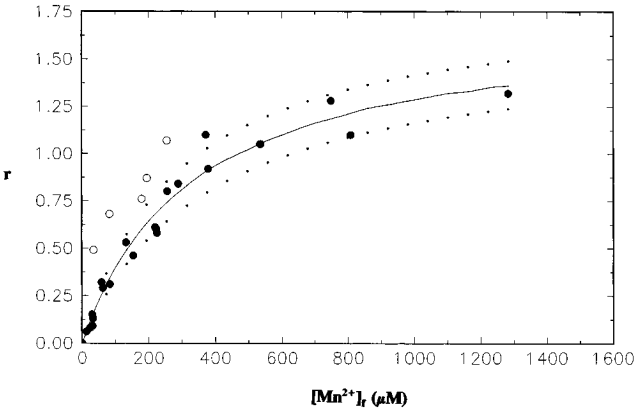

FIGURE 8: Mn^{2+} binding to the wild-type enzyme in the absence of GTP measured by flow-dialysis and by EPR under the same conditions as for wild-type enzyme in Figure 2. Open circles represent flow-dialysis data and closed circles EPR data. The solid curve is a nonlinear least-squares fit to the EPR data, and dotted curves denote the range corresponding to one standard deviation in n and K_d resulting from the nonlinear least-squares fit.

the values of n and K_d obtained in the presence of nucleotides are in the same range as those determined from EPR, and that the effect of nucleotides on the binding of Mn^{2+} to the enzyme is small.

DISCUSSION

We have explored by EPR and flow-dialysis using Mn^{2+} the possibility that the two essential Asp residues are the sites of metal binding. The transcription data show that Mn^{2+} can substitute for Mg^{2+} as a transcription activator, thereby assuring us that the EPR and flow-dialysis results are transcriptionally relevant. In addition, Mg^{2+} competes for the Mn^{2+}-binding site at a significantly higher concentration as observed in the EPR competition experiments, consistent with the transcription data. These differences between Mg^{2+} and Mn^{2+} fit with general observations concerning the properties of these two metal ions, and reinforce the argument that the ions are binding at the same site on the protein.

In our transcription studies, Mn^{2+} can substitute for Mg^{2+} as the metal ion transcription activator, and in all case that we have studied, the Mn^{2+} concentration necessary for optimal enzyme activity is less than the optimal Mg^{2+} concentration. When varying concentrations of Mn^{2+} were added to the transcription reaction containing 30 mM Mg^{2+}, the added Mn^{2+} caused slight enhancement of the transcription rate (see Results; Tables 2, 3, and 4; and Figure 6). These results are contrary to earlier reports that Mn^{2+} does not replace Mg^{2+} in a transcription reaction (Chamberlin & Ring, 1973) and that added Mn^{2+} in a transcription reaction containing Mg^{2+} inhibits transcription (Chamberlin & Ring, 1973; Coleman, 1983). The reason for these differences is not clear; however, the experimental conditions are very different.

The crystal structure of T7 RNA polymerase at 3.3 Å did not provide information on the metal ion binding sites since no divalent cations were present in the crystal. It was only suggested that Mg^{2+} may bind near the catalytically critical D537 and D812 side chains (Sousa et al., 1993). Consequently, we use the results of the present study, analogy to DNA polymerase structure, and prior results on metal binding to other biomolecules to postulate a metal-binding environment.

The results of the EPR experiments indicate that not only the wild-type T7 RNA polymerase but also the Asp single mutants (D537N; D537E; D812N; D812E) bind two Mn^{2+} with a single dissociation constant, within experimental error. Dissociation constants for the mutants are larger than for the wild-type enzyme (Table 1). In the double mutants, much weaker and probably nonspecific binding is observed. The possibility that the larger values of K_d for the mutants relative to the wild-type enzyme may be due to allosteric effects cannot be ruled out. However, the increase in K_d for both metal ions when a single potential metal-binding side chain is replaced by one with different coordination characteristics, the larger impact for double mutants than for single mutants, and the proximity of these two Asp groups in the X-ray crystal structure are most simply explained by proposing that both Asp carboxylates bind to both metal ions. The results of the flow-dialysis experiments show that the presence of nucleotides does not have a significant effect on the interaction of Mn^{2+} with the wild-type enzyme. A metal ion binding model consistent with our EPR and flow-dialysis data is depicted in Figure 4. This model departs from the more common bidentate bridging mode of carboxylate oxygens to the metal ions. Instead, it uses monodentate carboxylate oxygens of two Asp residues (wild-type) or one Asp and one Glu (Asp to Glu mutants) or the amide oxygen of an Asn and a carboxylate oxygen of an Asp (Asp → Asn mutants) to bridge the two metal ions. The metal to metal distance is calculated to be about 3.4 Å (Figure 4). If we assume that the two amino acids are not in the same plane, then the distance between the C_αs of two Asp (or Asp/Asn or Asp/Glu) residues is consistent with the values of the C_α to C_α distance of 5.2 Å calculated from the X-ray coordinates (Sousa et al., 1993) deposited in the Brookhaven Data Bank (Bernstein et al., 1977).

A monodentate carboxylate oxygen of an Asp residue bridging two metal ions has recently been observed in the active site of kidney bean purple acid phosphotase (Sträter et al., 1995), and the metal-to-metal distance in this crystal structure is 3.1 Å. The Zn^{2+} is coordinated by the amide oxygen of Asn201 analogous to the proposed binding in Figure 4. A monodentate carboxylate oxygen of Asp coordinating two metal ions was also postulated for cAMP-dependent protein kinase (Bossemeyer et al., 1993), and in the case of urease (Lippard, 1995), a carboxylate oxygen is coordinated to a metal ion and hydrogen-bonded to an acidic

Table 5: n and K_d Values for n Equivalent Noninteracting Sites, Obtained from Simulated Binding Isotherms Generated Using the Given K_{d1} and K_{d2} Values

K_{d1} (μM)	K_{d2} (μM)	K_d (μM)	n
339	160	226 ± 1.2	1.97 ± 0.01
339	339	339 ± 0.0	2.00 ± 0.00
339	800	479 ± 2.9	1.93 ± 0.01
339	1500	532 ± 7.5	1.76 ± 0.02
339	2500	523 ± 9.7	1.58 ± 0.02
339	3390	503 ± 9.7	1.47 ± 0.02

residue. In the active site of isopenicillin *N*-synthase (Roach *et al*., 1995), the amide oxygen of Gln330 was observed to coordinate Mn^{2+}.

An alternative to the proposed model with bridging Asp carboxylates is one in which each Asp coordinates only one of the bound metal ions. Mutating one of these residues to Asn or Glu will increase the K_d of the metal ion to which it binds, but should have little effect on the other metal ion. To test this hypothesis, we have considered a model with two intrinsic K_d's: one held at 339 μM, the wild-type value, and the other assigned values of 160, 339, 800, 2500, and 3400 μM. We have generated theoretical Scatchard plots for this model to evaluate the extent of deviations from linearity. The results show that deviations from linearity are perceptible, but allowing for experimental error, these deviations from linearity will not be detectable. We have then used nonlinear least-squares to fit the simulated binding isotherms, assuming n equivalent noninteracting sites. The n and K_d values obtained from these simulated isotherms (Table 5) can be compared to those obtained from EPR experiments (Table 1). Note that the apparent K_d increases by less than a factor of 2 when $K_{d2}/K_{d1} \sim 5$ and decreases slightly for larger ratios of intrinsic constants. However, the apparent number of binding sites decreases significantly from 2 for $K_{d2}/K_{d1} \sim 5$. This occurs because the two intrinsic dissociation constants begin to be resolved. This predicted behavior contrasts with what we observe (Table 1), in which n remains essentially 2 whereas K_d increases by factors of 2−5. Thus, our data indicate that the intrinsic dissociation constants for both sites, while not necessarily equal, both undergo significant increases upon mutation. This strongly supports a model in which both Asp537 and Asp812 are bridges between both metals.

There are precedents in the literature for bimetallic active sites in polymerases. A phosphoryl transfer mechanism involving two metal ions was proposed initially from the structure of the 3′−5′ exonuclease domain of Klenow fragment bound to a single-stranded DNA (tetranucleotide) and dTMP (Beese & Steitz, 1991). In this structure, the metal−metal distance was 3.9 Å, and the two metal sites were found to be different, one of them 5-coordinate and the other 6-coordinate. Some details of these metal-binding sites were hypothetical, with the 3′-OH ligand modeled and the liganding waters postulated. Based on this model, a polymerase mechanism was postulated (Steitz, 1993; Steitz *et al*., 1994).

In the crystal of rat polymerase β soaked in $MnCl_2$, two Mn^{2+} appeared about 4 Å apart coordinated to one Asp residue situated between the two metals ions, and the presence of dTTP did not significantly perturb the positions of the two Mn^{2+} (Davies *et al*., 1994). However it was suggested that the binding geometry of metals may differ when DNA is present. In the ternary complex of rat DNA polymerase β with a DNA template-primer and ddCTP (Pelletier *et al*., 1994), two metal ion sites were seen 4 Å apart, and the second metal ion was believed to enter the active site with the nucleotide substrate. It was observed that dNTP binding in the binary and ternary complexes differs (Sawaya et al., 1994). The crystal structures of the Klenow fragment complexed with dNTP and pyrophosphate (Beese et al., 1993) show these molecules binding in the polymerase domain near many of the amino acids whose mutation has an effect on catalysis (Polesky et al., 1990, 1992). The authors, however, urged caution in extrapolating the results from the binary complex to a model for the ternary complex.

Based on these cited studies and general background information from the literature, we interpret our results as being consistent with a model in which two metal ions, Mg^{2+} and/or Mn^{2+}, are coordinated to the carboxylate oxygen of the catalytically essential and conserved Asp537 and Asp812. It is to be emphasized that the EPR spectra do not directly imply any particular coordination environment for the metal ions, except that it is of low symmetry. The binding equilibria do not permit the preparation of samples in which Mn^{2+} is present only coordinated to the polymerase, and hence EPR measurements that would in such a case reveal the environment of the metal cannot be applied.

The bound metal ions may be involved in facilitating the removal of a proton from the 3′-OH group to attack the α-phosphorous, the alignment of the incoming nucleotide, and/or stabilization of the pentacoordinate transition state for transcription activation. The T7 RNA polymerase-catalyzed transcription mechanism is also consistent with an in-line mechanism; namely, the reaction proceeds with inversion of configuration at the α-phosphate (Griffiths et al., 1987). Recently, a remarkable rate enhancement ($\sim 10^{13}$) in phosphonate ester hydrolysis by two metal ions was reported (Tsubouchi & Bruice, 1994) in a model system. In all these cases involving two metal ion mechanisms, the details of metal participation may be different, but the general mechanistic aspects are similar.

The EPR data are generally in agreement with the transcription data using Mg^{2+} and Mn^{2+}. However, the K_d values of the metal ion complexes with the Asp mutants D537N and D812N obtained from the EPR experiments are at most 2−5 times the K_d value for the wild-type, whereas these mutants show no perceptible enzymatic activity. How can the small effect on the metal ion dissociation constants be reconciled with the drastic effect on enzyme activity? Four possibilities can be suggested. (1) Although the ability of the two Asp mutants, D537N and D812N, to bind the 22 bp template is not impaired (Osumi-Davis et al., 1992), the mutant enzymes may be incapable of forming open promoter complexes, thus causing enzymatic inactivation. (2) Asp537 and/or Asp812 may participate in the reaction in some role, in addition to metal ion binding. For example, they might act as a proton acceptor. This would be consistent with lack of activity in the Asp → Asn mutants, but significant activity in Asp → Glu mutants. Although this might account for the essential character of one Asp, it seems rather unlikely to be true for both Asp537 and Asp812. (3) The geometric requirements for stabilization of the transition state are generally different and usually much more stringent than those for ground states. Thus, small differences in the

positioning of metal ions, other ligands of the metal ions, water molecules, and other side chains could be induced by the mutations. These might have only small destabilizing effects on the metal ion−protein interactions, but could have much larger effects on the transition state stabilization. (4) Transcription requires that DNA and nucleotides are bound to the enzyme. Our studies of the metal ion affinities of the mutant enzymes have all been performed in the absence of nucleotides and template. Conformational differences in the transcriptionally active form of the enzyme may lead to dramatic differences in metal ion binding for Asp → Asn mutants that parallel the difference in kinetics.

ACKNOWLEDGMENT

We acknowledge the contribution of Professor Gareth Eaton for his critical reading of the manuscript and his suggestions and comments.

REFERENCES

Beese, L. S., & Steitz, T. A. (1991) *EMBO J. 10*, 25−33.
Beese, L. S., Friedman, J. M., & Steitz, T. A. (1993) *Biochemistry 32*, 14095−14101.
Bernstein, F. C., Koetzle, T. F., Williams, G. J. B., Meyers, E. F., Jr., Brice, M. D., Rodgers, J. R., Kennard, O., Shimanouchi, T., & Tasumi, M. (1977) *J. Mol. Biol. 112*, 535.
Bonner, G., Patra, D., Lafer, E. M., & Sousa, R. (1992) *EMBO J. 11*, 3767−3775.
Bonner, G., Lafer, E. M., & Sousa, R. (1994) *J. Biol. Chem. 269*, 25120−25128.
Bossemeyer, D., Engh, R. A., Kinzel, V., Ponstingl, H., & Huber, R. (1993) *EMBO J. 12*, 849−859.
Chamberlin, M., & Ring, J. (1973) *J. Biol. Chem. 248*, 2235−2244.
Cohn, M., & Townsend, J. (1954) *Nature (London) 173*, 1090−1091.
Coleman, J. E. (1983) *Zinc Enzymes* (Spiro, T. G., Ed.) pp 219−252, Wiley-Interscience, New York.
Davanloo, P., Rosenberg, A. H., Dunn, J. J., & Studier, F. W. (1984) *Proc. Natl. Acad. Sci. U.S.A. 81*, 2035−2039.
Davies, J. F., II, Almassy, R. J., Hostomska, Z., Ferre, R. A., & Hostomsky, Z. (1994) *Cell 76*, 1123−1133.
Delarue, M., Poch, O., Tordo, N., Moras, D., & Argos, P. (1990) *Protein Eng. 3*, 461−467.
Eaton, S. S., & Eaton, G. R. (1977) *Anal. Chem. 49*, 1277−1278.
Griffiths, A. D., Potter, B. V., & Eperon, I. C. (1987) *Nucleic Acids Res. 15*, 4145−4162.
Grodberg, G., & Dunn, J. J. (1988) *J. Bacteriol. 170*, 1245−1253.
Irving, H., & Williams, R. J. P. (1953) *J. Chem. Soc.*, 3192−3210.
Jacobo-Molina, A., Ding, J., Nanni, R. G., Clark, A. D., Jr., Lu, X., Tantillo, C., Williams, R. L., Kamer, G., Ferris, A. L., Clark, P., Hizi, A., Hughes, S. H., & Arnold, E. (1993) *Proc. Natl. Acad. Sci. U.S.A. 90*, 6320−6324.
Knoll, D. A., Woody, R. W., & Woody, A-Y. M. (1992) *Biochim. Biophys. Acta 1121*, 252−260.
Kohlstaedt, L. A., Wang, J., Friedman, J. M., Rice, P. A., & Steitz, T. A. (1992) *Science 256*, 1783−1790.
Lippard, S. J. (1995) *Science 268*, 996−997.
Meirovitch, E., & Poupko, R. (1978) *J. Phys. Chem. 82*, 1920−1925.
Mildvan, A. S., & Cohn, M. (1966) *J. Biol. Chem. 241*, 1178−1193.
Mookhtiar, K. A., Peluso, P. S., Muller, D. K., Dunn, J. J., & Coleman, J. E. (1991) *Biochemistry 30*, 6305−6313.
Muise, O., & Holler, E. (1985) *Biochemistry 24*, 3618−3622.
Munsen, P. J. (1983) *Methods Enzymol. 92*, 543−576.
Norby, J. G., & Jensen, J. (1988) *Methods Enzymol. 156*, 191−201.
Ollis, D. L., Brick, P., Hamlin, R., Xuong, N. G., & Steitz, T. A. (1985) *Nature (London) 313*, 762−766.
O'Sullivan, W. J., & Cohn, M. (1966) *J. Biol. Chem. 241*, 3104−3115.
Osumi-Davis, P. A., de Aguilera, M. C., Woody, R. W., & Woody, A-Y. M. (1992) *J. Mol. Biol. 226*, 37−45.
Osumi-Davis, P. A., Sreerama, N., Volkin, D., Middaugh, C. R., Woody, R. W., & Woody, A-Y. M. (1994) *J. Mol. Biol. 237*, 5−19.
Pelletier, H., Sawaya, M. R., Kumar, A., Wilson, S. H., & Kraut, J. (1994) *Science 264*, 1891−1903.
Polesky, A. H., Steitz, T. A., Grindley, N. D. F., & Joyce, C. M. (1990) *J. Biol. Chem. 265*, 14579−14591.
Polesky, A. H., Dahlberg, M. E., Benkovic, S. J., Grindley, N. D. F., & Joyce, C. M. (1992) *J. Biol. Chem. 267*, 8417−8428.
Raskin, C. A., Diaz, G., Joho, K., & McAllister, W. T. (1992) *J. Mol. Biol. 228*, 506−515.
Roach, P. L., Clifton, I. J., Fülöp, V., Harlos, K., Barton, G. J., Hajdu, J., Andersson, I., Schofield, C. J., & Baldwin, J. E. (1995) *Nature 375*, 700−704.
Sawaya, M. R., Pelletier, H., Kumar, A., Wilson, S. H., & Kraut, J. (1994) *Science 264*, 1930−1935.
Sousa, R., Chung, Y. J., Rose, J. P., & Wang, B.-C. (1993) *Nature 364*, 593−599.
Steitz, T. A. (1993) *Curr. Opin. Struct. Biol. 3*, 31−38.
Steitz, T. A., Smerdon, S. J., Jäger, J., & Joyce, C. M. (1994) *Science 266*, 2022−2025.
Sträter, N., Klaubunde, T., Tucker, P., Witzel, H., & Krebs, B. (1995) *Science 268*, 1489−1492.
Tsubouchi, A., & Bruice, T. C. (1994) *J. Am. Chem. Soc. 116*, 11614−11615.
Womack, F. C., & Colowick, S. P. (1973) *Methods Enzymol. 27*, 464−471.

BI952037F